PNAS PLUS

Hhip haploinsufficiency sensitizes mice to age-related emphysema

Taotao Lao[a], Zhiqiang Jiang[a], Jeong Yun[a,b], Weiliang Qiu[a], Feng Guo[a], Chunfang Huang[a], John Dominic Mancini[a], Kushagra Gupta[b], Maria E. Laucho-Contreras[b,c], Zun Zar Chi Naing[a], Li Zhang[b], Mark A. Perrella[b,d], Caroline A. Owen[b,c], Edwin K. Silverman[a,b], and Xiaobo Zhou[a,b,1]

[a]Channing Division of Network Medicine, Brigham and Women's Hospital and Harvard Medical School, Boston, MA 02115; [b]Division of Pulmonary and Critical Care Medicine, Department of Medicine, Brigham and Women's Hospital and Harvard Medical School, Boston, MA 02115; [c]Chronic Obstructive Pulmonary Disease Program, The Lovelace Respiratory Research Institute, Albuquerque, NM 87108; and [d]Pediatric Newborn Medicine, Brigham and Women's Hospital and Harvard Medical School, Boston, MA 02115

Edited by Gregg L. Semenza, The Johns Hopkins University School of Medicine, Baltimore, MD, and approved June 17, 2016 (received for review February 24, 2016)

Genetic variants in Hedgehog interacting protein (*HHIP*) have consistently been associated with the susceptibility to develop chronic obstructive pulmonary disease and pulmonary function levels, including the forced expiratory volume in 1 s (FEV_1), in general population samples by genome-wide association studies. However, in vivo evidence connecting *Hhip* to age-related FEV_1 decline and emphysema development is lacking. Herein, using *Hhip* heterozygous mice ($Hhip^{+/-}$), we observed increased lung compliance and spontaneous emphysema in $Hhip^{+/-}$ mice starting at 10 mo of age. This increase was preceded by increases in oxidative stress levels in the lungs of $Hhip^{+/-}$ vs. $Hhip^{+/+}$ mice. To our knowledge, these results provide the first line of evidence that *HHIP* is involved in maintaining normal lung function and alveolar structures. Interestingly, antioxidant *N*-acetyl cysteine treatment in mice starting at age of 5 mo improved lung function and prevented emphysema development in $Hhip^{+/-}$ mice, suggesting that *N*-acetyl cysteine treatment limits the progression of age-related emphysema in $Hhip^{+/-}$ mice. Therefore, reduced lung function and age-related spontaneous emphysema development in $Hhip^{+/-}$ mice may be caused by increased oxidative stress levels in murine lungs as a result of haploinsufficiency of *Hhip*.

HHIP | emphysema | COPD | aging | oxidative stress

Aging (senescence) increases vulnerability to age-associated diseases, such as chronic obstructive pulmonary disease (COPD), the third leading cause of death in the United States (1). COPD is also strongly influenced by cigarette smoke (CS) and genetic predisposition (2, 3).

Genome-wide association studies (GWAS) have successfully identified susceptibility loci for many complex diseases in the last decade (4, 5). However, understanding the biology underlying these GWAS associations remains a major challenge (6, 7). Mechanistic studies on novel susceptibility genes in complex traits, including COPD and pulmonary function levels, may provide insights into disease pathogenesis and thus highlight potential targets for therapy. Through GWAS, the chromosome 4q31 Hedgehog interacting protein (*HHIP*) locus has been consistently identified in COPD (8–10) and in spirometric measures, including the forced expiratory volume in 1 s (FEV_1) and ratio of FEV_1 to forced vital capacity in general population samples (11–14). Hhip represses hedgehog signaling by competitive binding with three Hedgehog (HH) ligands: Sonic Hedgehog, Indian Hedgehog, and Desert Hedgehog (15). Deletion of the *Hhip* gene in mice is neonatally lethal because of defective branching in the lung (14, 15). The reduced expression of *HHIP* in COPD lungs, and reduced enhancer activity associated with COPD risk alleles at the *HHIP* locus (16), suggested a protective role of *HHIP* in COPD pathogenesis.

Cellular redox (reduction-oxidation) homeostasis is necessary to protect cells from internal and external environmental stresses, thus maintaining normal cellular functions. During aging, reactive oxygen species (ROS) production and oxidant burden increase in lungs, contributing to parenchymal lung destruction and emphysema (17, 18). Pulmonary emphysema may result from accelerated and premature aging of the lungs because of cellular senescence (19), consistent with the observation that most COPD patients develop disease at advanced ages. Deficiency of cellular guardian genes, such as *SIRT1* (sirtuin 1) (20) and *TLR4* (Toll receptor 4) (21), leads to spontaneous pulmonary emphysema in murine models because of increased oxidative stress and accelerated aging.

We have previously shown that *Hhip* heterozygous knockout mice ($Hhip^{+/-}$) developed more severe emphysema than wild-type littermates when exposed to CS (22), suggesting that *HHIP* protects lung cells from environmental stressors, such as CS exposure. To extend our findings and understand the roles of *HHIP* in regulating lung function in nonsmokers, $Hhip^{+/-}$ mice were evaluated in an aging model. Lung quasi-static compliance, pressure–volume (PV) flow loops, and lung morphology were assessed over time, and molecular mechanisms by which *Hhip* regulates lung redox homeostasis and determines susceptibility to age-related emphysema were investigated.

Results

***Hhip* Haploinsufficiency Leads to Spontaneous Age-Dependent Airspace Enlargement.** Given that the *HHIP* locus is consistently associated with pulmonary function levels in the general population, we

Significance

Genome-wide association studies (GWAS) have been very successful in discovering genetic loci associated with complex traits. However, only few studies applied murine models to investigate how GWAS genes contribute to human lung diseases. Motivated by GWAS linking Hedgehog interacting protein (*HHIP*) to emphysema and impairments in lung function, this study demonstrated that $Hhip^{+/-}$ mice developed spontaneous emphysema and lung function impairment over time. Moreover, emphysema, associated with increased oxidative stress in $Hhip^{+/-}$ lungs, was prevented by treating the mice with the antioxidant, *N*-acetyl cysteine (NAC). This post-GWAS functional study connects aging-related diseases, molecular mechanisms, and potential therapy in a genetic haploinsufficient murine model, which may lead to improvements in understanding pathophysiologic concepts of alveolar loss related to aging.

Author contributions: T.L., E.K.S., and X.Z. designed research; T.L., Z.J., J.Y., F.G., C.H., J.D.M., K.G., M.E.L.-C., Z.Z.C.N., and L.Z. performed research; M.A.P. and C.A.O. contributed new reagents/analytic tools; T.L., W.Q., C.A.O., and X.Z. analyzed data; and T.L. and X.Z. wrote the paper.

Conflict of interest statement: In the past three years, E.K.S. received honoraria and consulting fees from Merck, grant support and consulting fees from GlaxoSmithKline, and honoraria from Novartis.

This article is a PNAS Direct Submission.

[1]To whom correspondence should be addressed. Email: xiaobo.zhou@channing.harvard.edu.

This article contains supporting information online at www.pnas.org/lookup/suppl/doi:10.1073/pnas.1602342113/-/DCSupplemental.

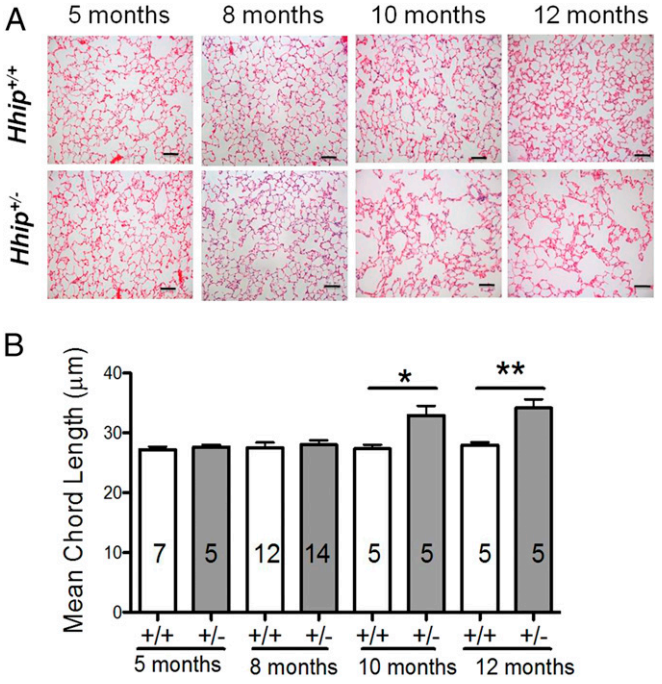

Fig. 1. Age-dependent airspace enlargement in *Hhip*$^{+/-}$ mice. (*A*) Histology of lung sections from *Hhip*$^{+/-}$ vs. wild-type littermate control mice (*Hhip*$^{+/+}$) at different ages as demonstrated by H&E staining. (Scale bars, 60 μm.) (*B*) Mean chord length (MCL) measurements on airspace size in murine lung sections from *Hhip*$^{+/+}$ (+/+) and *Hhip*$^{+/-}$ (+/–) mice. Means ± SEM shown in *B* are from 5 to 14 mice per group. **P* < 0.05 and ***P* < 0.01 by unpaired *t* test. There is a significant interaction between genotype and ages of mice by two-way ANOVA (*P* < 0.01).

assessed lung morphology and mechanics in *Hhip*$^{+/-}$ and *Hhip*$^{+/+}$ mice at different ages without smoke exposure. *Hhip*$^{+/-}$ mice have normal lung development (14) and normal distal airspace size at up to 8 mo of age. However, starting at 10 mo of age, *Hhip*$^{+/-}$ mice demonstrated significant age-dependent increases in airspace size in contrast to *Hhip*$^{+/+}$ mice (Fig. 1) (unpaired *t* test, $P < 0.01$), suggesting increased susceptibility of *Hhip*$^{+/-}$ mice to age-related airspace enlargement. There were also strong interactions between genotype and age of mice, suggesting genotype- and age-dependent airspace enlargement in murine lungs (Fig. 1*B*) (two-way ANOVA, $P < 0.01$).

***Hhip* Haploinsufficiency Accelerated Age-Dependent Lung Compliance Increases.** Consistent with airspace enlargement, *Hhip*$^{+/-}$ mice showed significantly increased lung compliance and decreased total lung elastance compared with age-matched *Hhip*$^{+/+}$ mice at 10 and 12 mo of age (Fig. 2 *A* and *B*) (unpaired *t* test, $P < 0.05$). Furthermore, *Hhip*$^{+/-}$ mice showed left shifts in the PV loops starting at 10 mo of age, suggesting that *Hhip* haploinsufficiency led to increased quasi-static lung compliance (Fig. 2*C*) (unpaired *t* test at each pressure point, $P < 0.05$). These age-related impairments in respiratory mechanics were associated with progressively reduced expression of *Hhip* in *Hhip*$^{+/+}$ murine lungs and even greater reductions in *Hhip* expression in *Hhip*$^{+/-}$ lungs during aging (Fig. S1) (23), supporting protective roles of *Hhip* during aging.

Increased Lymphoid Aggregates in the Lungs of *Hhip*$^{+/-}$ Mice During Aging. Aging lungs may exhibit signs of chronic inflammation (24), and *Hhip*$^{+/-}$ mice demonstrated increased numbers of lymphoid aggregates in lungs after chronic CS exposure (22); we therefore assessed lymphoid aggregates in murine lungs at different ages. The number of peri-bronchial lymphoid aggregates was significantly increased in *Hhip*$^{+/-}$ mice (Fig. 3 *A* and *B*) (unpaired *t* test, $P < 0.05$) at 10 and 12 mo of age compared with age-matched *Hhip*$^{+/+}$ mice. Consistently, the expression of CXCR3 (C-X-C chemokine receptor type 3) and CXCR5 were also significantly increased in *Hhip*$^{+/-}$ lungs at 10 mo of age as assessed by RT-PCR (Fig. 3 *C* and *D*) (unpaired *t* test, $P < 0.05$). CXCR5 is crucial for B-cell migration, whereas CXCR3 induces the migration of activated T cells into the lungs (25, 26). Interestingly, CXCL10 (C-X-C motif chemokine 10), a ligand for CXCR3, and MCP1 (monocyte chemotactic protein 1) also showed increased levels in *Hhip*$^{+/-}$ compared with *Hhip*$^{+/+}$ lungs at 8 mo of age (Fig. 3 *E* and *F*) (unpaired *t* test, $P < 0.05$). These results indicate increased recruitment of B and T lymphocytes into the lungs in *Hhip*$^{+/-}$ mice at 8–10 mo of age. However, total cell counts in bronchoalveolar lavage did not show significant difference between *Hhip*$^{+/-}$ and *Hhip*$^{+/+}$ mice at 10 mo of age (Fig. 3*G*).

Increased Levels of Matrix Metallopeptidases in the Lungs of *Hhip*$^{+/-}$ Mice. Matrix metallopeptidases (MMPs) promote emphysema development in both human COPD patients and murine emphysema models (27); thus, we compared levels of MMPs in lungs from *Hhip*$^{+/+}$ and *Hhip*$^{+/-}$ mice. MMP-9 protein levels were significantly increased in *Hhip*$^{+/-}$ lungs at 12 mo of age (Fig. S2*A*) (unpaired *t* test, $P < 0.05$). MMP-12 levels were significantly affected by *Hhip* genotype with a trend toward increased levels in *Hhip*$^{+/-}$ lungs (Fig. S2*B*) (two-way ANOVA, $P < 0.05$). Lung levels of the collagenase, MMP-8, also showed interaction between genotype and age time points (Fig. S2*C*) (two-way ANOVA, $P < 0.05$). However, no differences in levels of MMP-2 were detected in *Hhip*$^{+/-}$ and *Hhip*$^{+/+}$ mice at either 8 or 12 mo of age (Fig. S2*D*).

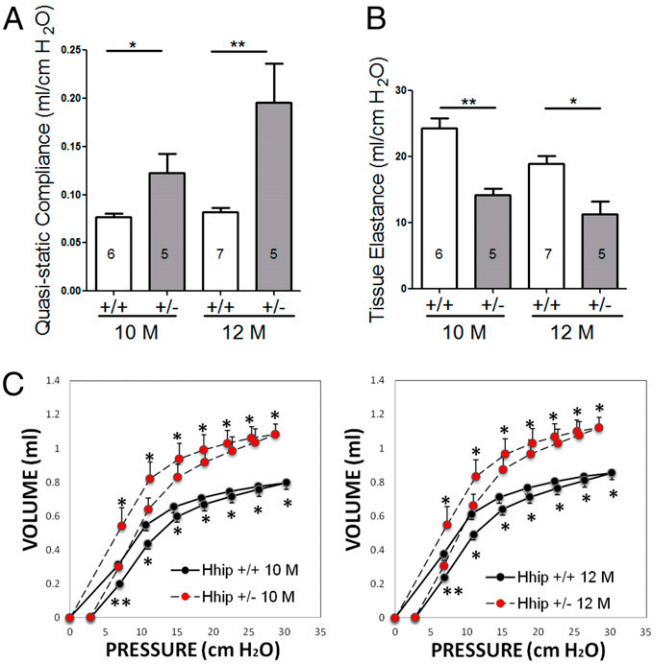

Fig. 2. Lung mechanics measurements in *Hhip*$^{+/+}$ and *Hhip*$^{+/-}$ mice at 10 and 12 mo (M) of age. (*A*) Lung compliance measurements. (*B*) Tissue elastance measurements. (*C*) Lung volume–pressure curve measurements. **P* < 0.05 and ***P* < 0.01 by unpaired *t* test at each pressure point to compare mean volume in *Hhip*$^{+/+}$ and *Hhip*$^{+/-}$ mice. *Hhip*$^{+/-}$ mice at 10 and 12 mo of age had left shifts in their pressure–volume curves compared with *Hhip*$^{+/+}$ mice at the same age, indicating that the *Hhip*$^{+/-}$ mice have higher quasi-static lung compliance. Means ± SEM are shown for each group (*n* = 5–7 mice per group).

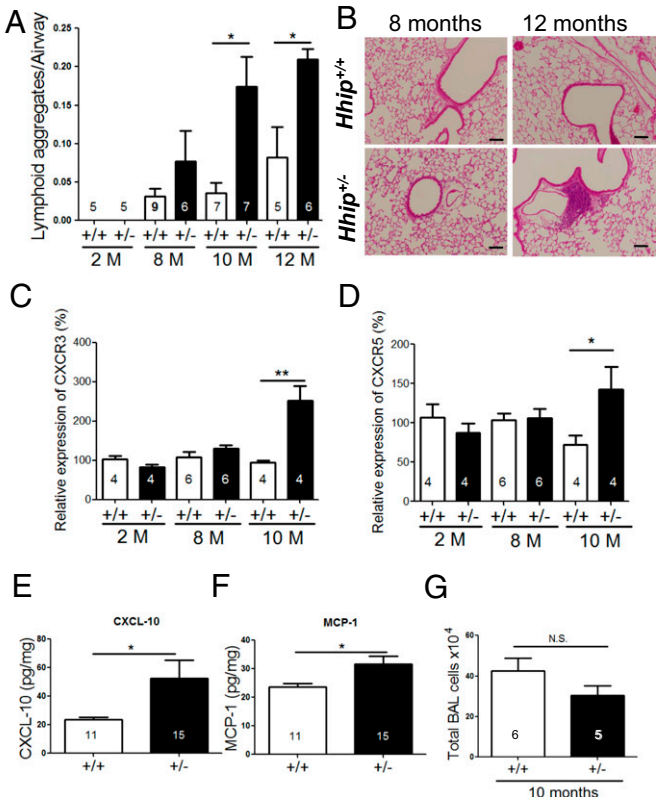

Fig. 3. Increased lymphoid aggregates in the lungs of *Hhip*$^{+/-}$ mice during aging. (*A*) Quantification of lymphoid aggregates per airway (mean internal diameter of 200–1,000 μm) in *Hhip*$^{+/+}$ mice (+/+) and *Hhip*$^{+/-}$ mice (+/–) at different ages. Data are means ± SEM from five to nine mice per group. (*B*) H&E staining in murine lungs. (Scale bars, 60 μm.) (*C* and *D*) Gene expression of CXCR3 and CXCR5 in lungs from *Hhip*$^{+/+}$ (+/+) and *Hhip*$^{+/-}$ (+/–) mice. Mean ± SEM are shown. (*E* and *F*) Measurements on CXCL10 and MCP1 levels in lungs from *Hhip*$^{+/+}$ (+/+) and *Hhip*$^{+/-}$ (+/–) mice at 8 mo (M) of age. Data are means ± SEM from 11 to 15 mice per group. (*G*) Total cell counts in bronchoalveolar lavage from mice at 10 mo of age. *$P < 0.05$; **$P < 0.01$ by unpaired *t* test. N.S., nonsignificant.

Increased Cell Death and Cell Senescence in *Hhip*$^{+/-}$ Lungs. As alveolar septal cell apoptosis contributes to emphysema development (28), we also measured cell death in lungs. Significantly increased cell death as assessed by TUNEL staining was detected in lungs from *Hhip*$^{+/-}$ mice compared with *Hhip*$^{+/+}$ mice at 8 mo of age (Fig. S3 *A* and *B*) (unpaired *t* test, $P < 0.05$). However, no difference in cell proliferation was detected in *Hhip*$^{+/-}$ vs. *Hhip*$^{+/+}$ lungs as assessed by *Ki*67 staining (Fig. S3 *C* and *D*). Furthermore, we assessed cellular senescence markers in murine lungs. Increased p53 and p21 levels were detected in *Hhip*$^{+/-}$ lungs compared with *Hhip*$^{+/+}$ lungs at 10 mo of age (Fig. S4) (unpaired *t* test, $P < 0.05$).

Increased Oxidative Burden in *Hhip*$^{+/-}$ Lungs. To identify pathways driving spontaneous emphysema in *Hhip*$^{+/-}$ mice, we assessed genes differentially expressed in 8-mo-old (preceding phenotypic changes) *Hhip*$^{+/-}$ and *Hhip*$^{+/+}$ murine lungs (22). All 48 up-regulated genes in *Hhip*$^{+/-}$ vs. *Hhip*$^{+/+}$ mice were significantly enriched in biological oxidation pathways by gene set enrichment analysis (false-discovery rate is 1.20E-04) (Table S1). A subset of selected genes validated by quantitative RT-PCR included Mt3 (metallothionein 3) and Adh7 (alcohol dehydrogenase 7) (Fig. S5 *A*–*D*). Increased expression of genes enriched in xenobiotic pathways suggested a pro-oxidant state in *Hhip*$^{+/-}$ murine lungs at 8 mo of age.

To further confirm that *Hhip*$^{+/-}$ mice have increased lung oxidative stress levels, we measured reduced glutathione (GSH) and oxidized GSH (GSSG) in lung lysates from *Hhip*$^{+/+}$ and *Hhip*$^{+/-}$ mice. A markedly lower GSH/GSSG ratio was found in lung lysates from 9-mo-old *Hhip*$^{+/-}$ mice compared with *Hhip*$^{+/+}$ mice (Fig. S5*E*) (unpaired *t* test, $P < 0.05$). Consistently, the antioxidant capacity in lungs showed a strong age-related reduction in *Hhip*$^{+/-}$ mice (Fig. S5*F*) (one-way ANOVA, $P < 0.01$).

Hhip, Expressed in Alveolar Type II Cells, Regulates Cellular Oxidant Stress. Immunofluorescence staining of lung sections revealed that Hhip colocalizes with SPC (surfactant protein C), a marker of alveolar type II (AT II) cells (Fig. 4*A*), with a reduced level of Hhip in *Hhip*$^{+/-}$ mice (Fig. 4*B*). However, no differences in the numbers of AT II cells (quantified by SPC staining) were detected between *Hhip*$^{+/-}$ and *Hhip*$^{+/+}$ mice at 2 mo of age (Fig. 4*C*).

We then assessed oxidative stress responses in AT II cells. Increased intracellular ROS levels were detected in AT II cells isolated from 9-mo-old *Hhip*$^{+/-}$ mice compared with cells from age-matched *Hhip*$^{+/+}$ mice (Fig. 4*D*) (unpaired *t* test, $P < 0.01$). Consistently, increased cell death rates were detected in AT II cells from *Hhip*$^{+/-}$ mice treated with H_2O_2 (Fig. 4*E*) (unpaired *t* test, $P < 0.05$).

HHIP Interacts with GSTP1 and Enhances Glutathione-Conjugating Activity. HHIP prevents the HH ligands from activating transcription factor Gli1 (29). However, AT II cells having minimal Gli1 expression are less likely to be responsive to HH ligands. To identify the potential molecular mechanisms by which HHIP contributes to redox homeostasis in AT II cells, we applied two screening approaches: (*i*) we searched for cellular proteins that interact with HHIP using affinity purification followed by MS; and (*ii*) we used a PCR array-based assay to measure expression changes of genes related to oxidative stress pathways in AT II cells derived from *Hhip*$^{+/-}$ mice and age-matched *Hhip*$^{+/+}$ mice.

First, in HEK 293 cells transfected with a C-terminal Flag/HA-tagged HHIP construct, HHIP-interacting proteins were visualized by silver staining after immunoprecipitation (IP) with anti-HA antibody (Fig. 5*A*). Through MS, 239 proteins were identified as cellular interacting proteins of HHIP after background subtraction of proteins identified from vector-transfected cells. Among novel HHIP interacting partners, we detected the presence of GST π 1 (GSTP1), a GST family member that catalyzes the conjugation of GSH with electrophilic compounds to fulfill its detoxification function. First, we confirmed the interaction between HHIP and GSTP1 by IP in HEK 293 cells transfected with Flag/HA-tagged HHIP. Compared with full-length HHIP, HHIP$^{1–193}$ that contains a frizzled domain on the N terminus of HHIP maintains its interaction with GSTP1 but HHIP$^{194–592}$ did not (Fig. 5*B*). Furthermore, overexpression of the full-length HHIP (but not the GSTP1 binding-deficient HHIP$^{194–592}$ mutant) improved cell viability (Fig. S6*A*), increased GSTP1 activity (Fig. S6*B*), and reduced intracellular ROS accumulation in Beas-2B cells treated with H_2O_2 (Fig. 5*C*), suggesting that the interaction between GSTP1 and HHIP promotes GSTP1 activity and thereby reduces lung oxidative stress levels. Second, we assessed where HHIP interacts with GSTP1 inside cells. Intracellular HHIP was detectable in the mitochondria of AT II cells (Fig. S7*A*), whereas GSTP1 interacts with HHIP mainly in the mitochondrial fraction of Beas-2B cells, which was enhanced after H_2O_2 treatment (50 μM for 1 h) (Fig. 5*D*). To determine whether HHIP modulates GSTP1 function, we measured GST enzymatic activity in AT II cells derived from *Hhip*$^{+/-}$ and *Hhip*$^{+/+}$ mice at 9 mo of age. We detected significantly lower GST activity in AT II cells derived from *Hhip*$^{+/-}$ vs. *Hhip*$^{+/+}$ mice (Fig. 5*E*), suggesting that HHIP promotes the activity of GST in murine AT II cells. We also detected increased mitochondrial-derived ROS, represented by increased mitoSOX staining in AT II cells from *Hhip*$^{+/-}$ compared with *Hhip*$^{+/+}$ mice at 9 mo of age (Fig. S7*B*), suggesting a functional impacts of *Hhip* on mitochondria by limiting mitochondrial-derived ROS accumulation in AT II cells.

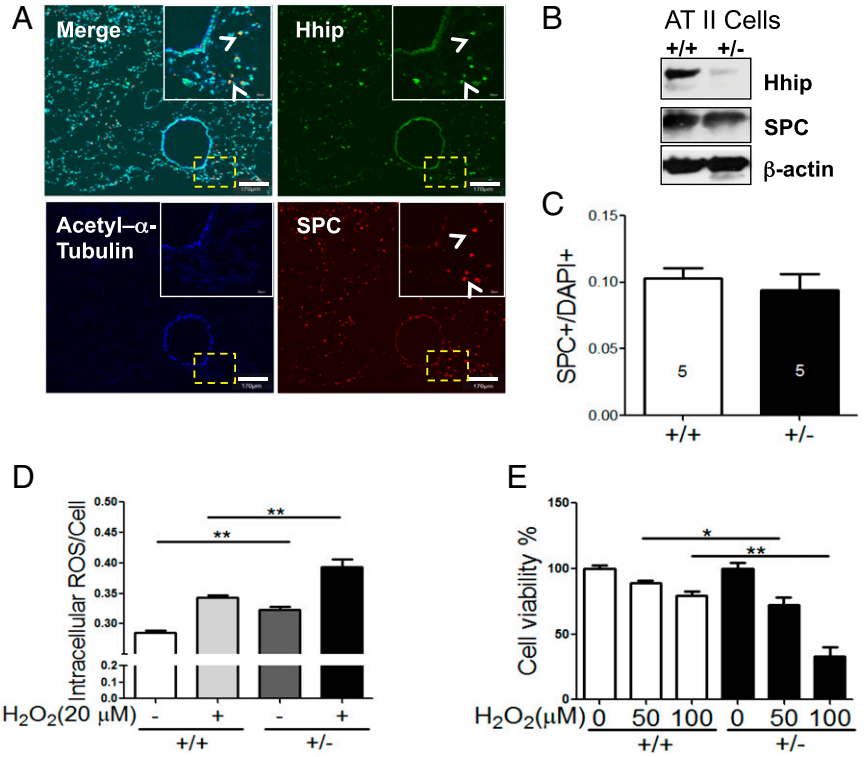

Fig. 4. Hhip regulates oxidative stress in murine alveolar type II (AT II) epithelial cells. (*A*) Immunofluorescence staining of Hhip in murine lungs from a wild-type C57BL/6 mouse. White arrowheads indicated colocalization of Hhip and SPC in AT II cells. (Scale bars, 170 μm.) (*B*) Immunoblotting of Hhip in AT II isolated from $Hhip^{+/+}$ (+/+) and $Hhip^{+/-}$ (+/–) mice. (*C*) Quantification of SPC^{+} cells in lungs from age-matched $Hhip^{+/-}$ and $Hhip^{+/+}$ mice at 2 mo of age (five mice per group). (*D*) Intracellular ROS levels in AT II cells under H_2O_2 treatment. $^{**}P < 0.01$, unpaired *t* test. (*E*) Cell viability measurements in AT II cells treated with H_2O_2 (0, 50, and 100 μM) for 18 h. Means ± SEM shown are from six replicate wells for each condition. $^{*}P < 0.05$ and $^{**}P < 0.01$ by unpaired *t* test.

Expression Profiling of Genes in the Oxidative Stress Pathway in AT II Cells. To further identify additional mechanisms by which HHIP regulates redox homeostasis in AT II cells, we screened 84 known genes related to the oxidative stress pathway by RT-PCR (Mouse Oxidative Stress RT^2 Profiler PCR Array, Qiagen) in AT II cells derived from $Hhip^{+/-}$ and $Hhip^{+/+}$ mice at 7 mo of age. Of 84 genes, 24 were differentially expressed in AT II cells from $Hhip^{+/-}$ compared with cells from $Hhip^{+/+}$ mice (fold change > 1.5) (Fig. S8 *A* and *B*). Three of these 24 genes, uncoupling protein 2 and 3 (UCP2 and UCP3) and neutrophil cytosolic factor 1 (NCF1) were significantly increased in AT II cells from $Hhip^{+/-}$ mice (Fig. S8*C*), suggesting oxidative status is increased in $Hhip^{+/-}$ AT II cells. Among these 24 genes, expression of four antioxidant genes were reduced in AT II cells from $Hhip^{+/-}$ mice (Table S2): dual oxidase 1 (Duox1), glutathione peroxidase 6 (Gpx6), prostaglandin-endoperoxide synthase 1 (Ptgs1), and recombination activating gene 2 (Rag2), suggesting that HHIP promotes other antioxidant functions beyond its capability to bind to and increase the activity of GSTP1.

Antioxidant Treatment in $Hhip^{+/-}$ Mice. We next asked whether increased oxidant levels induced age-related lung destruction and increased lung compliance in $Hhip^{+/-}$ mice. We added NAC (*N*-acetyl-cysteine) (30–33), a thiol antioxidant that previously was shown to improve age-related emphysema in murine models (21), to the drinking water of $Hhip^{+/-}$ and $Hhip^{+/+}$ mice at 5 mo of age. When mice were harvested at 10 mo of age, airspace sizes were similar in $Hhip^{+/-}$ and $Hhip^{+/+}$ mice treated with NAC, in marked contrast to mice without NAC treatment (Fig. 6 *A* and *B*). NAC treatment also significantly reduced lung compliance in $Hhip^{+/-}$ mice compared with age-matched untreated $Hhip^{+/-}$ mice (Fig. 6*C*) (two-way ANOVA, $P < 0.05$). These functional and morphological improvements in $Hhip^{+/-}$ murine lungs were associated with significant reductions in the number of lymphoid aggregates (Fig. 6*D*), as well as the activity of collagenase (Fig. S9*A*) and elastase (Fig. S9*B*) in $Hhip^{+/-}$ mice treated with NAC compared with untreated $Hhip^{+/-}$ mice. As expected, NAC treatment reduced oxidative stress levels in $Hhip^{+/-}$ mice as assessed by reductions in oxidation of total protein in lung lysates from $Hhip^{+/-}$ mice (Fig. 6 *E* and *F*). These findings supported the notion that the increased oxidant burden in $Hhip^{+/-}$ murine lungs may drive the development of emphysema and impair pulmonary function during aging through promoting inflammation and MMPs activity, which was inhibited by antioxidant NAC treatment (Fig. S10).

Discussion

COPD is more prevalent in the elderly (34) and lung function levels normally decline with aging. Understanding the biological mechanisms underlying aging-induced FEV_1 decline and emphysema development is an urgent unmet need. Motivated by human GWAS studies showing that *HHIP* is associated with both COPD affection status in case-control studies and FEV_1 levels in general population samples (12, 13), we demonstrate that *HHIP* protects aging-related airspace enlargement and increases in lung compliance in mice. Reduction in *HHIP* expression in COPD lungs (16), as well as in lungs of aging rodents (23), increases susceptibility to develop emphysema during aging. Furthermore, reduced antioxidant capacity and increased oxidant levels in $Hhip^{+/-}$ mice preceded emphysema development.

HHIP inhibits the HH pathway, a critical lung developmental pathway, through preventing three ligands from binding to its receptor, protein patched homolog 1, and eventually activating Gli1 (29). However, age-related emphysema in $Hhip^{+/-}$ mice might depend on a noncanonical HH pathway given that the HH pathway was regarded as an antagonist of aging in Alzheimer's disease and

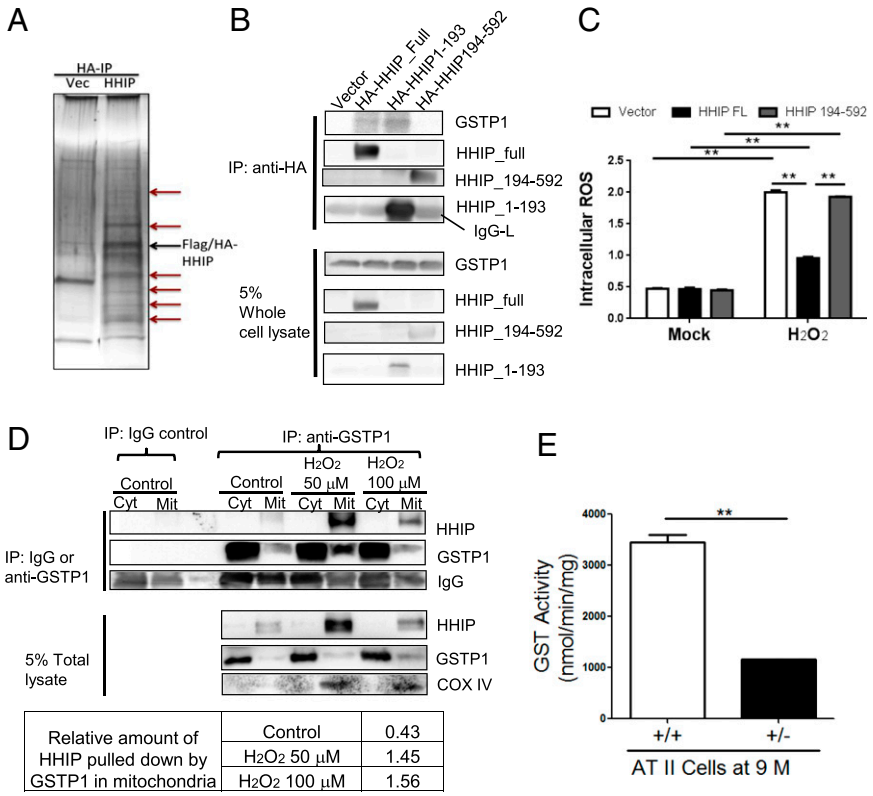

Relative amount of HHIP pulled down by GSTP1 in mitochondria		
	Control	0.43
	H_2O_2 50 μM	1.45
	H_2O_2 100 μM	1.56

Fig. 5. HHIP interacts with GSTP1 and enhances glutathione-conjugating activity. (*A*) Affinity purification of cellular protein complexes associated with Flag/HA-tagged HHIP (indicated by the black arrow) in HEK 293 cells as indicated by the red arrows. (*B*) IP of HHIP by anti-HA antibody in HEK 293 cells transfected with HHIP full length, $HHIP^{1–193}$, or $HHIP^{194–592}$ deletion mutant followed by immunoblotting (IB) with indicated antibodies. IgG-L, IgG light chain. (*C*) Intracellular ROS measurements in Beas-2B cells transfected with empty vector, full-length HHIP, or $HHIP^{194–592}$ deletion mutant after H_2O_2 treatment (200 μM for 12 h). (*D*) IP of GSTP1 in mitochondrial (Mit) and cytosol (Cyt) fractions by anti-GSTP1 or isotype IgG (control) antibody in Beas-2B cells treated with H_2O_2 (50 μM or 100 μM) for 1 h. Relative amount of HHIP to GSTP1 in the Mit-IP portions was shown in the bottom table. (*E*) GST activity measurements in AT II cells from 9-mo-old $Hhip^{+/-}$ and $Hhip^{+/+}$ mice. $^{**}P < 0.01$, unpaired *t* test.

diabetes (35) because of its critical roles in organ-specific stem cells (36, 37). We would expect a slower aging process because of partial de-repression of the HH pathway in $Hhip^{+/-}$ mice (22), whereas we observed accelerated aging-associated emphysema and increased cellular senescence in $Hhip^{+/-}$ mice. By searching for additional interacting proteins of HHIP, we identified GSTP1, a detoxification gene, which protects murine lung epithelial cells from H_2O_2-induced cell death (38). Therefore, the interaction between HHIP and GSTP1 in the cellular mitochondrial fraction suggests that HHIP may reduce oxidative stress by binding to and possibly increasing the activity of GSTP1. Interestingly, overexpressing GSTP1 in *Caenorhabditis elegans* extended its lifespan (39), suggesting a potential antiaging role of GSTP1, consistent with reduced GSTP1 activity in $Hhip^{+/-}$ mice.

Based on its interaction with GSTP1, HHIP may have an autonomous effect in AT II cells. However, $Pdgfr\alpha^{+}$ (platelet-derived growth-factor receptor α) mesenchymal cells but not endothelial cells and alveolar type I cells in the alveolar space also express HHIP (Fig. S11). Therefore, increased cell death and senescence detected in lungs from $Hhip^{+/-}$ mice may result from a combination of autonomous and paracrine effects in multiple cell types. Although more work is needed to characterize autonomous and paracrine effects of HHIP in lungs during aging, it is noteworthy that the increased oxidant burden and increased lymphoid aggregates accompanied by lung function abnormalities in adult $Hhip^{+/-}$ mice recapitulate those seen in human COPD patients carrying risk alleles in the *HHIP* GWAS locus (16, 22).

Senile lungs also exhibit increased inflammation that is likely pathologically important for the development of COPD, including increased levels of CXCR3 and CXCR5 to promote migration of B and T lymphocytes (24). Consistent with increased levels of cytokines, lymphoid aggregates, previously associated with severe emphysema in human COPD lungs (40), were also detected in lungs from $Hhip^{+/-}$ mice. An increased number of lymphoid aggregates may contribute to the greater airspace enlargement observed in $Hhip^{+/-}$ mice as (*i*) lymphoid aggregate number and size correlate with emphysema severity in human COPD patients (41); (*ii*) activated T lymphocytes (which are present in lymphoid aggregates) not only secrete MMPs (42) that can promote lung destruction, but also induce greater MMP production by macrophages (43); (*iii*) B cells (also present in lymphoid aggregates) promote CS-induced emphysema in mice (44); and (*iv*) B-cell products (autoantibodies) have been linked to emphysema in CS-exposed mice and human COPD patients (45, 46). Thus, *Hhip* may protect mice from spontaneous airspace enlargement in mice by inhibiting adaptive immunity (including lymphoid aggregates formation).

The cause of reduced levels of *Hhip* in lungs during aging, which may include reduced numbers of AT II cells during aging or reduced number of transcripts of HHIP in each AT II cell, needs further investigation. Nonetheless, a moderate reduction of *Hhip* in $Hhip^{+/-}$ mice was sufficient to provoke oxidative stress, lymphoid aggregates, alveolar loss, lung function abnormalities, and cellular senescence related to emphysema at 10 mo of age, suggesting that normal levels of *Hhip* are critical to maintain lung homeostasis.

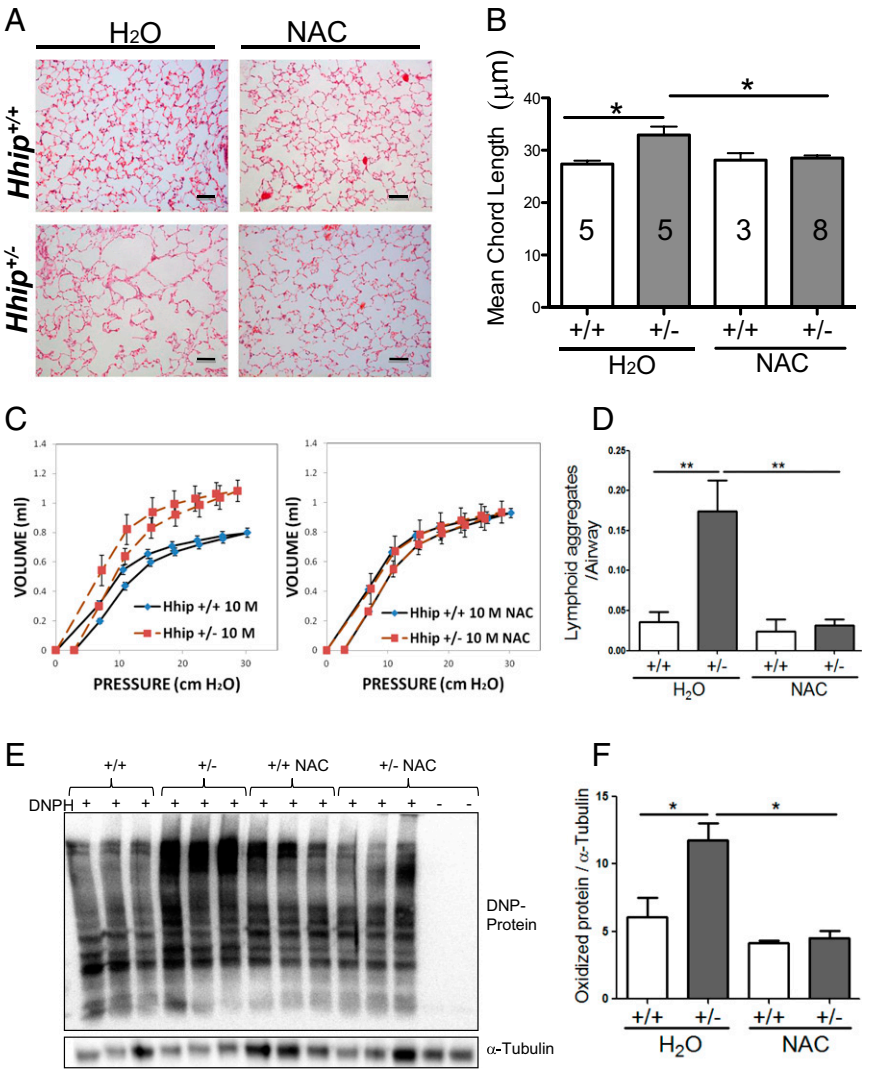

Fig. 6. Improved lung function and reduced airspace in *Hhip*$^{+/-}$ mice by antioxidant treatment. H&E staining of lung sections (*A*) and MCL measurements (*B*) on murine lung sections from *Hhip*$^{+/+}$ and *Hhip*$^{+/-}$ mice at 10 mo of age with or without NAC treatment for 5 mo. (Scale bars, 60 μm.) (*C*) Lung volume–pressure measurements. (*D*) Quantifications on lymphoid aggregates per airway in *Hhip*$^{+/+}$ and *Hhip*$^{+/-}$ mice at 10 mo of age treated with NAC or H_2O. $^{**}P < 0.01$, unpaired *t* test. (*E*) Protein oxidation measurements by Oxyblot. DNPH, 2,4-dinitrophenylhydrazine. (*F*) Densitometry quantifications on oxidized protein relative to α-Tubulin. Means ± SEM shown from three mice per group. $^{*}P < 0.05$, unpaired *t* test.

However, linking HHIP with aging definitively will require further comprehensive and sophisticated investigations. Therefore, we conclude that HHIP is important for maintaining lung homeostasis, but its plausible role in aging more generally will need additional evidence. Focusing on earlier age time points is instrumental to identify molecular pathways that serve as potential drivers for phenotypic changes in *Hhip*$^{+/-}$ lungs. Thus, we only used mice with maximum age of 18 mo in this study, unlike most other traditional aging studies.

Oxidative stress has been a therapeutic target for multiple diseases. Despite the well-accepted contribution of oxidative stress to pulmonary emphysema, the efficacy of antioxidant therapy in pulmonary disease has been controversial (27, 47), possibly because of genetic complexity in COPD patients. Given that *Hhip*$^{+/-}$ mice, which mimic human *HHIP* risk allele carriers with respect to *HHIP* expression levels, clearly derived more benefit from NAC treatment for pulmonary morphology and lung function improvement than *Hhip*$^{+/+}$ mice, additional studies are needed to determine whether COPD patients carrying *HHIP* risk alleles benefit more from antioxidant therapies.

Our results herein, coupled with our recent finding that *Hhip* protected mice from CS-induced emphysema (22), support the hypothesis that *Hhip* is essential for maintaining lung homeostasis during the aging process in response to environmental insults by protecting cells from oxidative stress-induced injury. Our studies expand knowledge about the molecular mechanisms by which *HHIP* contributes to age-related decline in lung function in humans. These new insights into aging-related emphysema may eventually facilitate the development and testing of more targeted therapies to reduce morbidity in aging subjects carrying risk variants at the *HHIP* locus by limiting decline in FEV_1 during aging.

Materials and Methods

Full experimental procedures and any associated references are available in *SI Materials and Methods*.

Animals. *Hhip*$^{+/-}$ mice in C57BL/6J background were described previously (22). This study was performed in strict accordance with the recommendations in the *Guide for the Care and Use of Laboratory Animals* (48) of the National Institutes of Health.

Airspace Size Analysis. For alveolar morphometric analysis, at least 15 images per mouse lung were randomly taken for analysis using methods described previously (22). Images were processed using Scion imaging software and analyzed for mean alveolar chord length (49).

Statistical Analysis Methods. We used two-way ANOVA analyses followed by Student two-sample unpaired *t* tests. See details in *SI Materials and Methods*.

ACKNOWLEDGMENTS. We thank Drs. Augustine M. K. Choi (Weill Cornell Medical College) and Xingbin Ai (Brigham and Women's Hospital) for their helpful discussions about this project. Funding of this project was provided by National Institutes of Health Grants R01 HL075478, P01 HL105339, and R01HL111759 (to E.K.S.), R01HL127200 and R33 HL120794 (to X.Z.), and R01 AI111475-01 and R21 HL111835 (to C.A.O.); the Flight Attendants Medical Research Institute CIA123046 (to C.A.O.); and Brigham and Women's Hospital and Lovelace Respiratory Research Institute Research Consortium (to C.A.O.).

1. Miniño AM, Xu J, Kochanek KD (2010) Deaths: Preliminary data for 2008. *Natl Vital Stat Rep* 59(2):1–52.
2. McCloskey SC, et al. (2001) Siblings of patients with severe chronic obstructive pulmonary disease have a significant risk of airflow obstruction. *Am J Respir Crit Care Med* 164(8 Pt 1):1419–1424.
3. Silverman EK, et al. (1998) Genetic epidemiology of severe, early-onset chronic obstructive pulmonary disease. Risk to relatives for airflow obstruction and chronic bronchitis. *Am J Respir Crit Care Med* 157(6 Pt 1):1770–1778.
4. Gibson G (2010) Hints of hidden heritability in GWAS. *Nat Genet* 42(7):558–560.
5. Manolio TA (2010) Genomewide association studies and assessment of the risk of disease. *N Engl J Med* 363(2):166–176.
6. Freedman ML, et al. (2011) Principles for the post-GWAS functional characterization of cancer risk loci. *Nat Genet* 43(6):513–518.
7. Juran BD, Lazaridis KN (2011) Genomics in the post-GWAS era. *Semin Liver Dis* 31(2): 215–222.
8. Pillai SG, et al.; ICGN Investigators (2009) A genome-wide association study in chronic obstructive pulmonary disease (COPD): Identification of two major susceptibility loci. *PLoS Genet* 5(3):e1000421.
9. Soler Artigas M, et al.; SpiroMeta Consortium (2011) Effect of 5 genetic variants associated with lung function on the risk of COPD, and their joint effects on lung function. *Am J Respir Crit Care Med* 184(7):786–795.
10. Nakamura H (2011) Genetics of COPD. *Allergol Int* 60(3):253–258.
11. Soler Artigas M, et al.; International Lung Cancer Consortium; GIANT Consortium (2011) Genome-wide association and large-scale follow up identifies 16 new loci influencing lung function. *Nat Genet* 43(11):1082–1090.
12. Repapi E, et al.; Wellcome Trust Case Control Consortium; NSHD Respiratory Study Team (2010) Genome-wide association study identifies five loci associated with lung function. *Nat Genet* 42(1):36–44.
13. Hancock DB, et al. (2010) Meta-analyses of genome-wide association studies identify multiple loci associated with pulmonary function. *Nat Genet* 42(1):45–52.
14. Chuang PT, Kawcak T, McMahon AP (2003) Feedback control of mammalian Hedgehog signaling by the Hedgehog-binding protein, Hip1, modulates Fgf signaling during branching morphogenesis of the lung. *Genes Dev* 17(3):342–347.
15. Chuang PT, McMahon AP (1999) Vertebrate Hedgehog signalling modulated by induction of a Hedgehog-binding protein. *Nature* 397(6720):617–621.
16. Zhou X, et al. (2012) Identification of a chronic obstructive pulmonary disease genetic determinant that regulates HHIP. *Hum Mol Genet* 21(6):1325–1335.
17. Karrasch S, Holz O, Jörres RA (2008) Aging and induced senescence as factors in the pathogenesis of lung emphysema. *Respir Med* 102(9):1215–1230.
18. Rahman I (2005) Oxidative stress in pathogenesis of chronic obstructive pulmonary disease: Cellular and molecular mechanisms. *Cell Biochem Biophys* 43(1):167–188.
19. Tuder RM, Petrache I (2012) Pathogenesis of chronic obstructive pulmonary disease. *J Clin Invest* 122(8):2749–2755.
20. Yao H, et al. (2012) SIRT1 protects against emphysema via FOXO3-mediated reduction of premature senescence in mice. *J Clin Invest* 122(6):2032–2045.
21. Zhang X, Shan P, Jiang G, Cohn L, Lee PJ (2006) Toll-like receptor 4 deficiency causes pulmonary emphysema. *J Clin Invest* 116(11):3050–3059.
22. Lao T, et al. (2015) Haploinsufficiency of Hedgehog interacting protein causes increased emphysema induced by cigarette smoke through network rewiring. *Genome Med* 7(1):12.
23. Misra V, et al. (2007) Global expression profiles from C57BL/6J and DBA/2J mouse lungs to determine aging-related genes. *Physiol Genomics* 31(3):429–440.
24. Aoshiba K, Nagai A (2007) Chronic lung inflammation in aging mice. *FEBS Lett* 581(18):3512–3516.
25. Moser B (2015) CXCR5, the defining marker for follicular B helper T (TFH) cells. *Front Immunol* 6:296.
26. Van Raemdonck K, Van den Steen PE, Liekens S, Van Damme J, Struyf S (2015) CXCR3 ligands in disease and therapy. *Cytokine Growth Factor Rev* 26(3):311–327.
27. Owen CA (2005) Proteinases and oxidants as targets in the treatment of chronic obstructive pulmonary disease. *Proc Am Thorac Soc* 2(4):373–385; discussion 394–375.
28. Park JW, Ryter SW, Choi AM (2007) Functional significance of apoptosis in chronic obstructive pulmonary disease. *COPD* 4(4):347–353.
29. Ingham PW, Nakano Y, Seger C (2011) Mechanisms and functions of Hedgehog signalling across the metazoa. *Nat Rev Genet* 12(6):393–406.
30. de Boer WI, Yao H, Rahman I (2007) Future therapeutic treatment of COPD: Struggle between oxidants and cytokines. *Int J Chron Obstruct Pulmon Dis* 2(3):205–228.
31. Barnes PJ (2008) Frontrunners in novel pharmacotherapy of COPD. *Curr Opin Pharmacol* 8(3):300–307.
32. de Batlle J, et al. (2010) Dietary modulation of oxidative stress in chronic obstructive pulmonary disease patients. *Free Radic Res* 44(11):1296–1303.
33. Firuzi O, Miri R, Tavakkoli M, Saso L (2011) Antioxidant therapy: Current status and future prospects. *Curr Med Chem* 18(25):3871–3888.
34. Thannickal VJ, et al. (2015) Blue journal conference. Aging and susceptibility to lung disease. *Am J Respir Crit Care Med* 191(3):261–269.
35. Dashti M, Peppelenbosch MP, Rezaee F (2012) Hedgehog signalling as an antagonist of ageing and its associated diseases. *BioEssays* 34(10):849–856.
36. Neureiter D (2012) New in Hedgehog signaling: A possible role in aging, and chronic degenerative and inflammatory diseases? (Comment on DOI 10.1002/bies.201200049). *BioEssays* 34(10):828–829.
37. Petrova R, Joyner AL (2014) Roles for Hedgehog signaling in adult organ homeostasis and repair. *Development* 141(18):3445–3457.
38. Fletcher ME, et al. (2015) Influence of glutathione-S-transferase (GST) inhibition on lung epithelial cell injury: Role of oxidative stress and metabolism. *Am J Physiol Lung Cell Mol Physiol* 308(12):L1274–L1285.
39. Ayyadevara S, et al. (2005) Lifespan and stress resistance of *Caenorhabditis elegans* are increased by expression of glutathione transferases capable of metabolizing the lipid peroxidation product 4-hydroxynonenal. *Aging Cell* 4(5):257–271.
40. Hogg JC, et al. (2004) The nature of small-airway obstruction in chronic obstructive pulmonary disease. *N Engl J Med* 350(26):2645–2653.
41. Polverino F, et al. (2015) B cell-activating factor. An orchestrator of lymphoid follicles in severe chronic obstructive pulmonary disease. *Am J Respir Crit Care Med* 192(6): 695–705.
42. Oviedo-Orta E, Bermudez-Fajardo A, Karanam S, Benbow U, Newby AC (2008) Comparison of MMP-2 and MMP-9 secretion from T helper 0, 1 and 2 lymphocytes alone and in coculture with macrophages. *Immunology* 124(1):42–50.
43. Maeno T, et al. (2007) CD8+ T cells are required for inflammation and destruction in cigarette smoke-induced emphysema in mice. *J Immunol* 178(12):8090–8096.
44. John-Schuster G, et al. (2014) Cigarette smoke-induced iBALT mediates macrophage activation in a B cell-dependent manner in COPD. *Am J Physiol Lung Cell Mol Physiol* 307(9):L692–L706.
45. Lee SH, et al. (2007) Antielastin autoimmunity in tobacco smoking-induced emphysema. *Nat Med* 13(5):567–569.
46. Feghali-Bostwick CA, et al. (2008) Autoantibodies in patients with chronic obstructive pulmonary disease. *Am J Respir Crit Care Med* 177(2):156–163.
47. Kirkham PA, Barnes PJ (2013) Oxidative stress in COPD. *Chest* 144(1):266–273.
48. Committee on Care and Use of Laboratory Animals (1996) *Guide for the Care and Use of Laboratory Animals* (Natl Inst Health, Bethesda), DHHS Publ No (NIH) 85-23.
49. Laucho-Contreras ME, Taylor KL, Mahadeva R, Boukedes SS, Owen CA (2015) Automated measurement of pulmonary emphysema and small airway remodeling in cigarette smoke-exposed mice. *J Vis Exp* (95):52236.